Mat. Res. Soc. Symp. Proc. Vol. 720 © 2002 Materials Research Society



# The Ferroelectric Slab Waveguide: a Geometry for Microwave Components that Incorporate Ferroelectric Materials

Frank J. Crowne and Steven C. Tidrow
RF Electronics Division, Army Research Laboratory,
Adelphi, MD 20783-1197, U.S.A.

## ABSTRACT

A slab geometry, in which ferroelectric is inserted between two "cladding" layers with a microstrip electrode placed on top, is proposed as a way to integrate the properties of ferroelectric materials into microwave components. This structure distributes the propagating microwave fields between the ferroelectric and the cladding, so that the microwave dielectric constant is a weighted average of the dielectric constants of the two materials. It is shown that this geometry drastically reduces dissipation due to dielectric losses in the ferroelectric. In addition, by applying a dc bias to the microstrip line, the dielectric constant of the ferroelectric layer can be varied and with it the microwave properties of the structure.

## INTRODUCTION

Due to its lack of moving parts and potential for conformal installation on vehicles, missiles and aircraft, the electrically scannable (E-scan) antenna is an important weapon in the arsenal of the Army's Future Combat Systems [1]. Most approaches to designing such antennas involve some type of phased array, in which beam steering is implemented by phase shifters. It has long been known that ferroelectric materials can be used to make such components, since they can provide voltage-controlled phase shifts by virtue of their nonlinear dielectric response.

Our recent in-house efforts on E-scan antennas at the Army Research Laboratory has centered on a true-time-delay approach to generating the antenna phase shifts, in which a tapped delay line, usually some sort of microwave transmission line, is used to phase the antenna signals by sampling a nondispersive propagating wave at equal intervals along its path. If the delay line is uniform, it is easy to show that an array phased in this way has a far-field pattern whose main lobe points at an angle $\theta_{MB}$ given by

$$\theta_{MB} = \sin^{-1}\left(\frac{D\sqrt{\varepsilon}}{d}\right) \tag{1}$$

where $D$ is the spacing between taps, $d$ is the distance between array radiators, and $\varepsilon$ is the dielectric constant of the delay line. If $\varepsilon$ is frequency independent, the angle $\theta_{MB}$ is also, so that broadband signals can be transmitted without causing the beam to move. In addition, if the transmission line is a microstrip line on a ferroelectric substrate, the field dependence of $\varepsilon$ makes it possible to steer the beam electrically with a single dc voltage between the strip and the ground plane.

However, this scheme turns out to be difficult to implement. In order to suppress coupling between array radiators, the spacing $d$ between them is usually $\lambda/2$, where $\lambda$ is

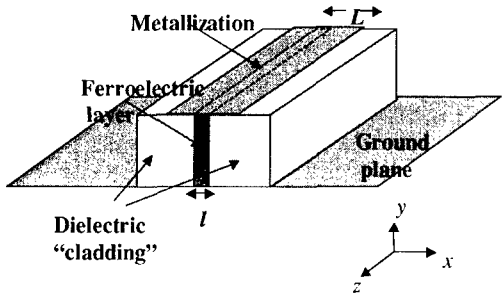


**Figure 1.** Ferroelectric slab structure.

the free-space wavelength of the carrier signal (typically a few centimeters down to a millimeter for our applications). Because dielectric constants are extremely high in ferroelectrics (1000 to 4000), satisfying Eq. (1) with an $\varepsilon$ of 1000 requires values of $D < \frac{d}{30}$, which puts the delay line taps quite close together. This causes arcing and cross talk, and makes the line difficult to manufacture.

## THEORY

Our approach to this problem is to replace the ferroelectric substrate with a guiding structure consisting of a thin slice of ferroelectric sandwiched between two "cladding" layers of low-$\varepsilon$ material. We have found that there is a frequency range within which a delay line based on this structure, which we call a *ferroelectric slab waveguide*, looks like a microstrip transmission line with an "effective" dielectric constant much lower than that of the ferroelectric. This ferroelectric-slab (FS) structure is shown in Fig. 1. By analogy with microstrip [2], let us assume that the region of the slab where the wave fields exist is bounded laterally at $x = \pm L/2$, by magnetic walls. Then for waves propagating along $z$ with propagation constant $q(\omega)$, the structure has a set of TE modes whose electric field $\mathrm{E}_y(x)$ is perpendicular to the ground plane and the microstrip metal. This field satisfies the wave equation:

$$\left(\partial_x^2 + \varepsilon(x)\frac{\omega^2}{c^2} - q^2\right)\mathrm{E}_y(x) = 0$$

where $\varepsilon(x) = \varepsilon_1$ for $x \in [l/2, L/2]$ and $\varepsilon_2$ for $x \in [0, l/2]$. In contrast to ordinary microstrip, these FS modes are nonuniform in $x$ due to the nonuniformity of $\varepsilon(x)$:

$$\begin{aligned}\mathrm{E}_y(x) &= A\cos K_2 x, && x \in [0, l/2] \\ &= A\left(\frac{\cosh K_2 l/2}{\cosh K_1 \Lambda/2}\right)\cosh K_1(L/2 - x), && x \in [l/2, L/2] \end{aligned} \qquad (2)$$

where $K_1^2 = q(\omega)^2 - \varepsilon_1 \frac{\omega^2}{c^2}$ and $K_2^2 = \varepsilon_2 \frac{\omega^2}{c^2} - q(\omega)^2$. Note that the field is oscillatory inside the ferroelectric and exponentially decaying outside in the cladding, like the field of an optical fiber mode [3]. Matching the field and its derivative at the boundary (which ensures continuity of the longitudinal magnetic field $H_z$), gives the relation

$$K_1 \tanh K_1 \Lambda / 2 = K_2 \tan K_2 l / 2 \tag{2a}$$

where $\Lambda = L - l$. Combining this with the equation

$$K_2^2 + K_1^2 = (\varepsilon_2 - \varepsilon_1) \frac{\omega^2}{c^2} \tag{2b}$$

and solving (2a) and (2b) numerically for $K_1$ and $K_2$ as a function of frequency, we obtain the propagation constant from $q(\omega)^2 = \varepsilon_1 \frac{\omega^2}{c^2} + K_1^2$.

Figure 2 shows the fundamental-mode electric field distribution of an FS with $L$ = .3 cm, $l$ = .005 cm, $\varepsilon_2$ = 1000, and $\varepsilon_1$ = 3.6, at two frequencies: $f$ = 3 GHz and $f$ = 50 GHz. At the lower frequency, the electric field is almost uniform across the structure, like the fundamental mode of an ordinary microstrip line. At $f$ = 50 GHz the confinement is apparent. The width of the ferroelectric is too small to see on this scale.

At low frequencies the mode problem can be solved analytically. Let us write $K_1 = \Xi \sin\phi$, $K_2 = \Xi \cos\phi$, where $\Xi^2 = (\varepsilon_2 - \varepsilon_1) \frac{\omega^2}{c^2}$. Then (2a) becomes

$$\sin\phi \cdot \tanh[(\Xi\Lambda/2)\sin\phi] = \cos\phi \cdot \tan[(\Xi l/2)\cos\phi] \tag{3}$$

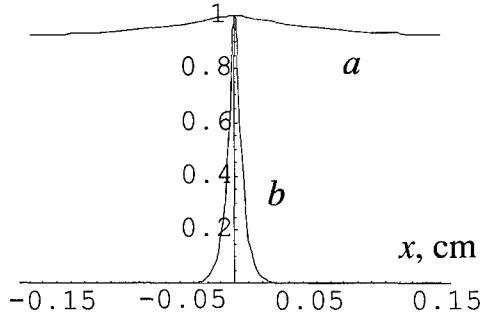


**Figure 2.** Fundamental modes of an FS at $f$ = 3 GHz ($a$) and 50 GHz ($b$). Structural parameters: $L$ = .3 cm, $l$ = .005 cm, $\varepsilon_2$ = 1000, and $\varepsilon_1$ = 3.6 [$A$ = 1 in Eq. (2)].

For small $\Xi$ (low frequencies), the tangents in (3) can be replaced by their arguments:

$$(\Xi\Lambda/2)\sin^2\phi = (\Xi l/2)\cos^2\phi. \tag{4}$$

Solving (4) gives $\cos\phi = \sqrt{\frac{\Lambda}{\Lambda+l}}$, $\sin\phi = \sqrt{\frac{l}{\Lambda+l}}$, and hence $K_1 = \frac{\omega}{c}\sqrt{\frac{l}{\Lambda+l}(\varepsilon_2-\varepsilon_1)}$, $K_2 = \frac{\omega}{c}\sqrt{\frac{\Lambda}{\Lambda+l}(\varepsilon_2-\varepsilon_1)}$, from which we obtain $q = \sqrt{\varepsilon_1\frac{\omega^2}{c^2}+K_1^2} = \frac{\omega}{c}\sqrt{\frac{\varepsilon_2 l+\varepsilon_1(L-l)}{L}}$.

In this limit the FS mode looks like the fundamental mode of an ordinary microstrip line on a substrate with dielectric constant equal to the weighted average of the dielectric constants of the two FS layers, i.e.,

$$\varepsilon_{eff} = \varepsilon_2\frac{l}{L}+\varepsilon_1(1-\frac{l}{L}), \tag{5}$$

which is derivable from a simple parallel capacitor model. Note that the electric field is uniform in this same limit, like that of microstrip.

As the frequency increases, the dispersion increases along with the confinement. Figure 3(*a*) shows the full dispersion relation for the structure described in Fig. 2. It is clear that there is a turnover point around 7 GHz where dispersionless propagation ends. This point is a critical design number for high-frequency devices, and must be identified for each structure. The perturbation analysis reveals that lack of dispersion depends on smallness of the quantity $\Xi$ defined above. Clearly there are two ways to make $\Xi$ small: either by operating at low frequencies or making the two dielectric materials have almost the same dielectric constant. The former method precludes high-frequency operation, while the latter is of no practical use because there are no perovskite ferroelectrics with small $\varepsilon_2$. However, a third limit in which the line is dispersionless is when $l$ is small but

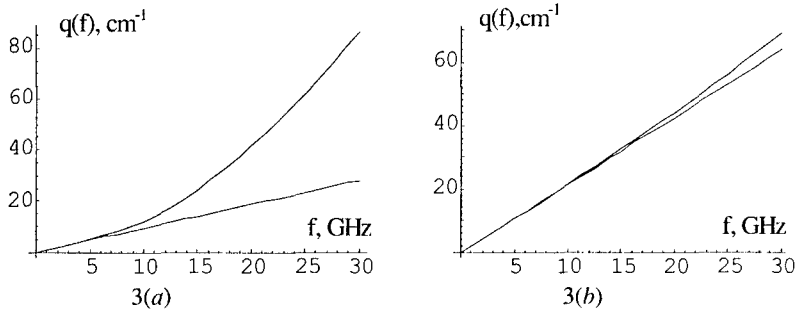


**Figure 3.** (*a*) Dispersion curve for FS with parameters listed in Fig. 2. Straight line: small-$\omega$ approximation ($\varepsilon_{eff}$ =20). (*b*) Dispersion curve for FS with parameters $L$ = .025 cm, $l$ = .0025 cm, $\varepsilon_2$ = 1000, and $\varepsilon_1$ = 3.6. Straight line: small-$\omega$ approximation ($\varepsilon_{eff}$ =103).

$\varepsilon_2$ is large. In this limit we have $K_1 \to 0$, which makes the electric field $E_y(x)$ independent of $x$, while at the same time $\varepsilon_{eff} \neq \varepsilon_2, \varepsilon_1$ as long as $l$ and $\varepsilon_2$ are chosen so that the product $\varepsilon_2 \frac{l}{L}$ remains sizable. Although $K_2$ does not vanish in this limit, the volume occupied by ferroelectric becomes too small to affect the propagation. Figure 3(*b*) shows a more useful dispersion curve, with a drastically narrower microstrip electrode. The effective dielectric constant is now very large, and the dispersionless regime now extends to almost 30 GHz.

Another advantage of the FS structure is that it can greatly reduce losses intrinsic to the ferroelectric by putting most of the electric field of the wave in the cladding, where losses can be miniscule. A perturbation analysis of the propagation [4] for a line with lossy ferroelectric gives the following expression for the complex propagation constant:

$$\tilde{q}_S \approx q(\omega) + j\frac{\omega^2}{2q(\omega)c^2}\int \varepsilon_I(x) E_y^2(x)dx$$

where $E_y(x)$ is the lossless mode shape given by Eq. (2) and $\varepsilon_I(x)$ is the imaginary part of $\varepsilon(x)$, which is nonzero only in the ferroelectric. This equation can be used to derive the loss tangent, and shows clearly how a small volume of ferroelectric leads to low losses.

Figure 4 shows the line losses for the structure defined in Fig. 2, for two values of ferroelectric loss tangent: a "fair" value (*a*) and a "good" value (*b*). Despite the fact that these numbers are terrible compared to ordinary dielectrics, the losses over a line a few centimeters long are extremely low. Note that these loss reductions were achieved with no sacrifice of "tuning," i.e., the rate of change of $\varepsilon$ with bias.

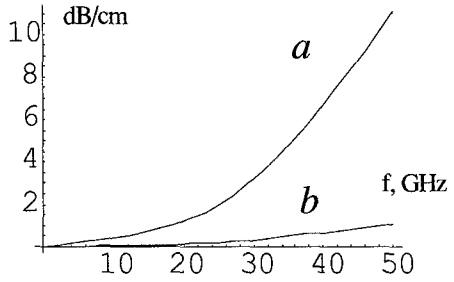


**Figure 4.** Line losses for an FS with structural parameters $L$ = .3 cm, $l$ = .005 cm, $\varepsilon_2$ = 1000, and $\varepsilon_1$ = 3.6, and ferroelectric loss tangents .03 (*a*) and .003 (*b*).

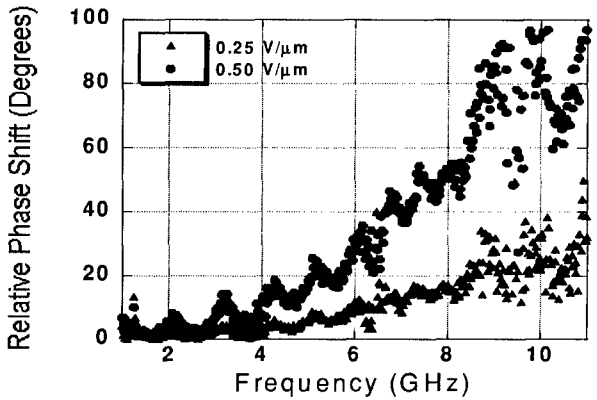


**Figure 5.** Phase shifts for untapped delay line.

## EXPERIMENT

Figure 5 shows preliminary experimental results for an untapped structure about 5 cm long. The *S*- parameter $S_{21}$, which corresponds to the transmission of a passive line, was measured in an HP network analyzer, and its phase was extracted. The peaks in the data correspond to resonances due to imperfect impedance matching at the end of the line. Reflections also suppress the phase shift, which should have been around 400 degrees for this structure. The remarkably small fields needed to change this linear trend attest to the promising nature of our approach. The percent change in $\varepsilon$ here was 10%.

## CONCLUSION

In conclusion, we believe that these microwave structures address and solve many of the problems that limit the use of ferroelectrics in microwave devices. We have begun to address some of the hard issues relating to impedance matching and aperture coupling of these lines to other microwave devices, e.g., patch antennas, and will report on our progress in a future publication.

## REFERENCES

1. S. Weiss, E. Adler, R. Dahlstrom, E. Viveiros, S. Tidrow, and F. J. Crowne, "A Low-Profile Architecture Implementation of an Electrically Scanned Antenna", *GOMAC2002*, Mar. 11-14, Monterey, CA, talk 13.2.
2. K. C. Gupta, R. Garg, and I. J. Bahl, *Microstrip Lines and Slotlines* (Artech House, Dedham, Massachusetts, 1979).
3. H. C. Casey Jr. and M. B. Panish, *Heterostructure Lasers: Part A* (Academic Press, New York, 1978).
4. A. Yariv, *Quantum Electronics* (2nd ed.,Wiley and Sons, New York, 1975), ch. 19.